

GT2016-56500

EXPERIMENTAL AND RANS NUMERICAL INVESTIGATION OF UNSTEADY STRUCTURES WITHIN THE RIM SEAL CAVITY IN THE PRESENCE OF PURGE MASS FLOW

Jason Town

Michael Averbach

Cengiz Camci

Department of Aerospace Engineering
The Pennsylvania State University
University Park, Pennsylvania, USA

ABSTRACT

Flow within the space between the rotor and stator of a turbine disk, an area referred to as the rim seal cavity, develops azimuthal velocity component from the rotor disk. The fluid within develops unsteady structures that move at a fraction of the rotor speed. A test is developed to measure the number of unsteady structures and the rotational speed at which they are moving in the rim seal cavity of an experimental research rig. Data manipulation was developed to extract the speed and the numbers of structures present using two fast response aerodynamic probes measuring static pressure on the surface of the stator side rim seal cavity. A computational study is done to compare measured results to a transient URANS. The computational simulation consists of 8 vanes and 10 blades, carefully picked to reduce error caused by blade vane pitch mismatch and to allow for the structures to develop correctly, and the rim seal cavity to measure the speed and number of the structures. The experimental results found 15 structures moving at 77.5% of the rotor speed, computational results are based on the size of the domain and guidance from the experimental results find 14.5 structures are moving at 81.7% rotor speed. The agreement represents the first known test of its kind and the first known agreement between computational and experimental work.

INTRODUCTION

Design of a turbine stage requires a gap between the non-moving stator wall and the rotating blade disk below the hub endwall surface. Air within the rim seal cavity begins to swirl

due to momentum imparted on the fluid through boundary layer interaction with the rotor disk. As the system of swirl develops, a system of high to low pressure cells moves within the rim seal cavity. The cells are identified by Cao et al. in a computational and experimental study of a two stage turbine [1]. The results conclude that there are eight unsteady structures moving 90% to 97% of the rotor speed. The structures present are independent from blade passing events.

Comparisons of three different types of computational studies are shown by Jakoby et al. [2]. The test that best represents the structures within the rim seal cavity is a complete 360 degree analysis. Three unsteady structures are found within the rim seal cavity, they are moving at 80% of the rotor speed. The geometry does not include the vanes or blades, but simulates them by imposing static pressure fields as their boundaries.

A computational test done by Julien et. al [3] includes a sector model of a model with 44 inlet guide vanes, and 58 rotor blades. The model shows approximately 30 structures are located within the rim seal cavity, they are moving at 90% of the rotor speed. Multiple tests are done at a variety of purge injection rates. Increasing the injection rate causes these structures to dissipate. The results are highly dependent on the design of the rim seal cavity.

A full unsteady 360 degree study based on the axial flow turbine test rig at Arizona State by Wang et al. [4] also has found evidence of the unsteady structures within the rim seal cavity. In this study the structures are found to correspond with ingress and egress out of fluid from the main stream to the rim seal

cavity. There are 12 cells move at 87% of the rotor speed, and also dissipate at higher purge flow rates. A rebuke by Mirzamoghadam et. al. was written claiming that the structures found may be a transient phenomenon that is caused by an insignificant number of revolutions of the rotor performed to resolve the case to a satisfactory solution [5].

The results concur that the cell size, shape, and speed are dependent on the design of the rim seal cavity and not the number of blades or vanes of the stage. A larger, more unobstructed cavity tends to lead toward larger pressure structures in smaller numbers that each take up greater azimuthal angles within the rim seal cavity. Current design is going toward smaller and more complex cavities than those tested by Cao and Jakoby et al. The new cavities designs have smaller and more numerous structures, each structure taking up a smaller azimuthal angle. These structures can be measured using fast response aerodynamic probes on the surface of the stator wall or the rotor disk, as Palaflox et. al. have done so [6]. They can also be simulated using a partial sector of the rim seal cavity if the sector is picked while keeping the number of structures in mind.

A complete annulus solution was found using a GPU powered URANS solver from ETH Zurich was studied by Basol et. al. [7]. Two different cases based on experimental geometries were used. In the first case (0.4% injection rate) no unsteady structures were found. In the case with a greater injection rate (0.9% of inlet mass flow) a separation bubble was found inside the cavity. The separation gave rise to unsteady structures within the rim seal cavity. Additionally, it was found that magnitude of the sinusoidal static pressure distribution is larger when a full 360° annular model than a model of 20° sector. Both models correctly predict the correct number of peaks and troughs.

The goal of this paper is to correctly measure the speed and number of structures within the rim seal cavity experimental using the Axial Flow Turbine Research Facility at The Pennsylvania State University. With reliable data from an experimental rig the next step is to use the results to guide our computational efforts. The ultimate goal being able to predict and accurately reproduce measured structures within the experimental rig with a computational methods.

NOMENCLATURE

AFTRF	Axial Flow Turbine Research Facility
NGV	Nozzle Guide Vane
θ_{diff}	Difference in degrees between transducers
t_{phase}	Difference in time between each peak across each transducer
ω_{rotor}	Rotor speed in radians per second
$N_{str\ total}$	Total number of structures identified
T_{sample}	Total sample time in seconds
Ω_{str}	Speed of the structure in radians per second
f_{str}	The frequency at which a structure passes by a transducer

N_{str}	Number of structures
$N_{str\ per\ second}$	Number of structures that pass by the transducer per second
f^*	Occurrences per rotor revolution
f	Frequency in Hertz
\dot{m}_{purge}	Mass flow rate injected into the rim seal cavity
$\dot{m}_{gaspath}$	Mass flow rate though the main gas path
RPM_{rotor}	Rotor speed in rotations per minute
T	Time to rotate the rotor one blade pitch
t	Elapsed time from start
$\theta_{peak,t}$	Peak location at time step
$\theta_{peak,t+1}$	Peak location at next time step
Δt	Computational time step

EXPERIMENTAL SETUP

The current configuration of the Axial Flow Turbine Research Facility (AFTRF) has 29 Nozzle Guide Vanes (NGV) and 36 rotor blades. It is a large scale (36.08 inch, 0.916 meter diameter), long duration, low speed turbine test stage that simulations state-of-the-art turbine blade, nozzle guide vanes, and rim seal cavity designs. A downstream, four stage axial flow fan system can provide a turbine with a 40 in of water (10000 Pa) pressure drop and a maximum flow rate of 10 kg/s. The inlet of the rig is left open to the atmosphere, there is minimal turbulence generation between the inlet of the rig and the turbine stage test section. Keeping turbulence low allows for greater understanding of the flow structures within the rotor itself by being able to isolate the effects and losses caused within the turbine.

The instantaneous performance of the rotor is monitored with an array of Pitot Probes, Kiel Probes, Validyne variable reluctance transducers (DP15), Validyne Carrier Demodulators (CD280), Scanivalve Corporation multiplexed differential pressure transducers (ZOC22B/32Px-2.5psid), Endevco Piezoresistive Pressure Sensors (8507C-1), and Endevco Amplifiers (Model 136). The rim seal cavity purge flow is supplied by a 300 psi lab air system. The purge injection system was originally designed in association with McClean. Results of the original experiments and designs can be found in two papers by McClean et. al. [8] [9]. The amount of air being supplied as purge is varied by a regulator and the mass flow rate is measured by an ASME calibrated orifice. All data is recorded using scripts from LabVIEW and National Instrument CompactDAQ instrumentation. A 16-Bit, 32 channel analog to digital converter from National Instruments (NI 9205) is used to measure voltages from the amplifiers and signal conditioners.

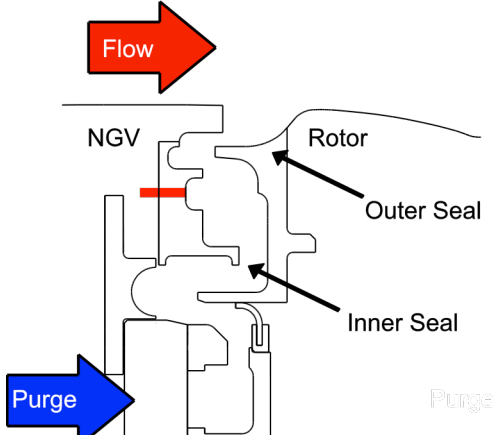


Figure 1: Rim Seal Cavity Geometry and Probe Location

The structures within the rim seal cavity affect ingress and egress patterns. Previous literature has shown that these structures have an alternating pattern of high and low static pressure. It is possible to calculate the speed and the number of structures present at any given time if at least two fast response probes are held at a known distance apart and can take data simultaneously. Two transducers manufactured by Endevco (model 8507C-1) are used to measure the structures. Representative geometry of the rim seal cavity is shown in Figure 1. The geometry is classified as a double radial seal, the red line represents the radial location of the flush mounted transducers. The cavity that the transducers are located next to is referred to as the buffer cavity, it is located between the outer and inner seals. Below the inner seal is a serpentine path that the injected purge flow must take to the rim seal cavity. This path is designed to fit within our experimental rig and is used for mixing and settling from periodic inlets located around the inner parameter of the annulus.



Figure 2: Flush Mounted Piezoresistive Pressure Transducers in Rim Seal Cavity, 5° Apart

The two pressure transducers are located 5° apart at the same radial location. The flush mounted piezoresistive pressure

transducers (Endevco model 8507C-1) are shown in Figure 2, where they are circled in red. Using our method at least two probes that can take data simultaneously are necessary to calculate the speed and number of structures within the rim seal cavity.

The unsteady structures in the rim seal cavity each have a unique pressure peak that must shift across the transducers at different times. The modern data acquisition system is set to take data from both piezoresistive pressure probes simultaneously. A known sample rate controlled by the internal clock of the data acquisition device is set so that a time difference can be calculated. The time difference is set by identifying the peak pressure of each unsteady structure and calculating the time difference via number of samples taken for that peak to pass from one transducer to another. This time difference can be used to calculate the fractional speed at which the structures are moving within the rim seal chamber as shown in Equation (1). In our case θ_{diff} is a known value of 5°.

$$\Omega_{str} = \frac{\theta_{diff}}{360} \frac{2\pi}{t_{phase} \cdot \omega_{rotor}} \quad (1)$$

Unsteady structures will rotate at a fraction of the rotor's angular velocity. Additionally, the number of structures can also be calculated. This can be done by dividing the number of structures that pass by the transducer each second and dividing it by the estimated frequency at which each unique structure passes by the transducer, as shown in Equation (2)

$$N_{str} = \frac{N_{str \text{ per second}}}{f_{str}} \quad (2)$$

$$N_{str \text{ per second}} = \frac{N_{str \text{ total}}}{T_{sample}}$$

$$f_{str} = \frac{\theta_{diff}}{360} \frac{1}{t_{phase}}$$

EXPERIMENTAL RESULTS

Two experimental test cases are shown in Table 1 along with target speed and purge flow rate percentage. Rotor speed is a corrected value based current atmospheric temperature. Typically the laboratory reached thermal equilibrium when the rotor was near 1430 RPM. Purge mass flow injection rate (\dot{m}_{purge}) is defined as the mass of the fluid being injected into the rim seal cavity externally. Two cases are set, one where no purge flow is used and the rate is at 0.00% of the main gas path flow rate. The target is at 0.25% main gas path flow rate, however a rate of 0.28% was easier to set experimentally. Measurements are done at 100,000 samples per second for 60 seconds in order to achieve a statistically significant number that can later be compared to computational RANS based solution.

Table 1

	RPM_{rotor}	$\dot{m}_{purge}/\dot{m}_{gaspath}$
Target	1430	0.25% or 0%
Case 1	1433	0.28%
Case 2	1433	0.00%

Test ‘Case 2’, where the purge flow injection rate was held at 0.00% of the inlet mass flow to the turbine, did not produce results that could be separated from the noise in the signal. As such, the results discussed in this paper will not include ‘Case 2’.

Experimental results are solved in the frequency spectrum. MATLAB employs transformations to convert the pressure signal into the frequency domain using Fast Fourier Transform (FFT) functions. Results are given as a function of occurrences per rotor revolution (f^*), the transform is given below.

$$f^* = \frac{2\pi f}{\omega_{rotor}} \quad (3)$$

MATLAB is optimized to work with FFTs, it quickly completes transforms by reducing the complexity of the equation. This is accomplished by adding zeros to the end of the equation until the length is a power of two. The total number of samples for a 60 second run at 100,000 samples per second is 6,000,000 samples. An optimization routine in MATLAB increases the length of the samples to 2^{23} , or 8,388,608 samples.

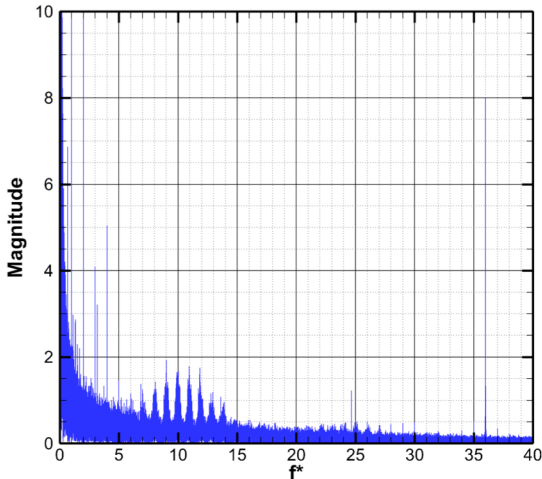


Figure 3: FFT of pressure Signals from Transducer 1, Case 1 (\dot{m}_{purge} is 0.28%)

Frequency domain results for the first can with a rotor speed of 1433 RPM and a purge mass flow rate of 0.28% of the main gas path for ‘Transducer 1’ can be seen in Figure 3. A large magnitude spike is recorded at $f^* = 36$. This is equal to the number of rotor blades and is equal to the blade passing frequency. The results indicate that the transducer is in an area of ingress. Thus it is more apt to measure the pressure field disturbances caused by the rotor blades as they pass. Frequencies

below five occurrences per revolution are understood to be noise.

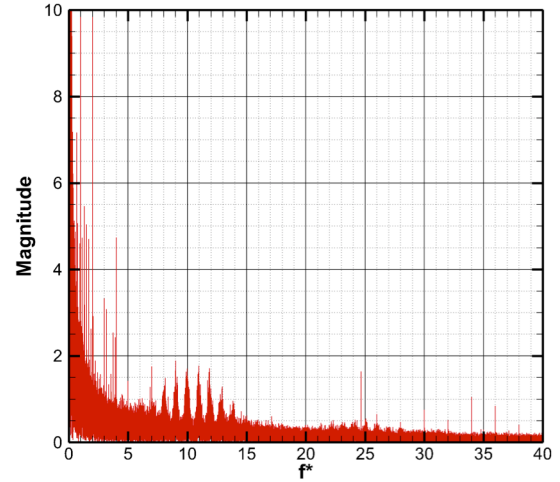


Figure 4: FFT of pressure Signals from Transducer 2, Case 1 (\dot{m}_{purge} is 0.28%)

The second transducer’s frequency spectrum results are shown in Figure 4. The blade passing frequency of 36 is not as pronounced as the first location results. The second transducer is not in a location of constant ingress, and the upstream rotor blade pressure field does not affect it as much. Frequencies below five occurrences per revolution are once again considered noise.

An enlarged version of each graph for the frequency range of 5 to 15 occurrences per revolution is shown in Figure 5. The signals that fall within this range are identified as the low frequency, unsteady structures within the rim seal cavity. A range of frequencies is identified as the unsteady structures because the structures may change shape, size, speed, and periodicity during operation. Additional investigation into how these evolve over time and further analysis of the data will reveal that the structures are unsteady even after a system reaches equilibrium.

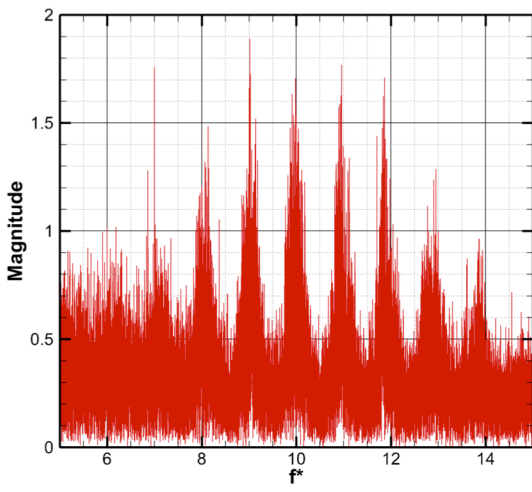
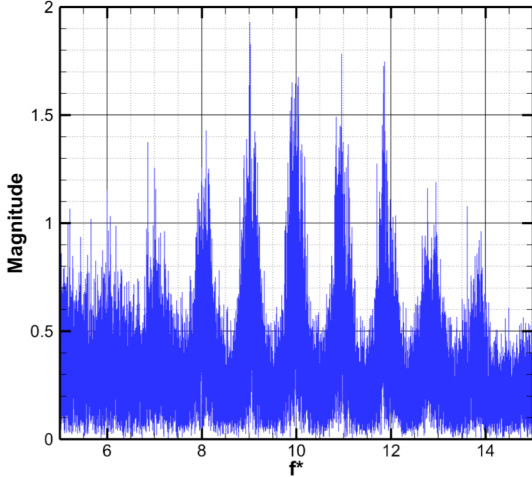


Figure 5: Enhanced View of Pressure Signals from Transducer 1 (Top, Blue) and Transducer 2 (Bottom, Red)

A Butterworth type bandpass filter with cutoff frequencies of 5.25 and 16.75 occurrences per revolution is used to isolate the unsteady structure signals from the rest of the measurements. The filtered results of the first case are shown in Figure 6, ‘Transducer 1’ is in blue on the top, and ‘Transducer 2’ is in red on the bottom. For ‘Case 1’ a clear set of similar signals is measured by each transducer. The signals are not caused by the blade or vane pressure fields (36 or 29 respectively). They are identified as unsteady structures within the rim seal cavity.

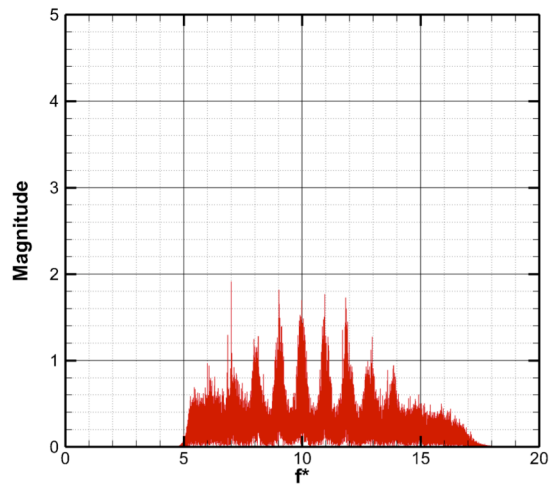
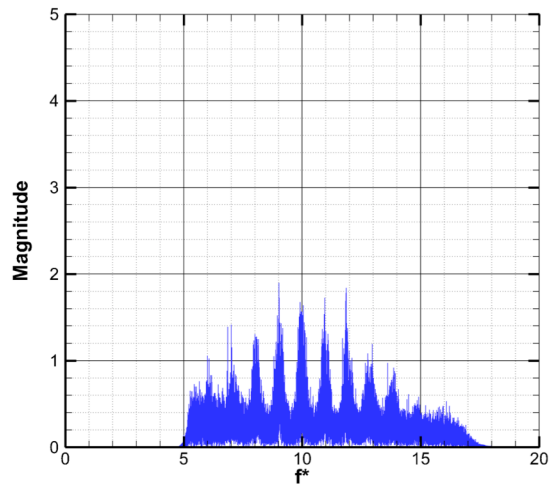


Figure 6: Butterworth Bandpass Filtered Pressure Signals from Transducer 1 (Top, Blue) and Transducer 2 (Bottom, Red)

Calculating the rotational speed and number of the unsteady structures is done by Equations (1) and (2). What is needed from the filtered data is the number of peaks present in the signal of each transducer and the time it takes for one peak to traverse between the two transducers. The location and number of peaks is found using the MATLAB function `findpeaks`. The function checks to see if a number is higher than a specified range of the immediate numbers around it. The range is set so that five numbers ahead and behind a value is checked to see which is greater. If the value is greater than all the numbers it is checked against, the value is identified as a peak.

A sample of the data consisting of approximately 20 blade passings is shown in Figure 7. The results show an instantaneous pressure value subtracted by the average value. The func-

tion (`findpeaks`) identified 16,547 peaks in ‘Transducer 1’ and 16,585 peaks in ‘Transducer 2’

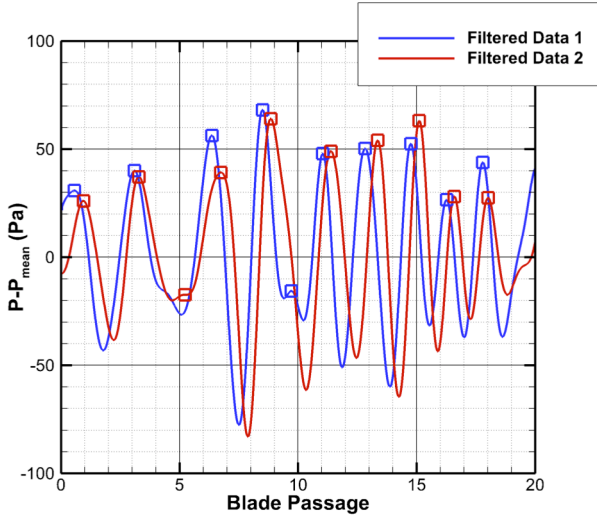


Figure 7: Filtered Pressure History with Identified Peaks

Identifying the peaks can be used to calculate the time it takes to move from one pressure port to another. The pressure peaks traverse from ‘Transducer 1’ to ‘Transducer 2’. There are 10 microseconds between each sample. Taking the number of samples between each peak and multiplying it by 10 microseconds results in the amount of time it takes for a pressure point to move between the two transducers.

The code looks for a pressure peak in the signal of ‘Transducer 1’, when found it calculates the number of samples and the time it takes for the same peak to occur in the signal of ‘Transducer 2’. This is not without flaw. For example in Figure 7 a peak is identified at 9 blade passings. There is not a corresponding peak in pressure signal ‘Transducer 2’. The code calculates the time difference between the peak at 9 blade passings from ‘Transducer 1’ and the peak at 13 blade passings from ‘Transducer 2’. This creates a large time difference and can skew the results to structures that are measured toward more slowly moving results. The second peak in ‘Transducer 1’ at 13 blade passings also uses the same peak at 13 blade passings in ‘Transducer 2’.

A histogram of the time it takes to traverse from the first transducer to the second is shown in Figure 8. The red represents the average of all the results, it is approximately 1000 microseconds to move between transducers. The average results is skewed by the code that cannot account for the missing pressure peaks in the second signal. The mode of the time difference is 750 microseconds. The mode is the value that is used for calculation of the speed and the number of structures. A more refined code will be able to reduce the data further.

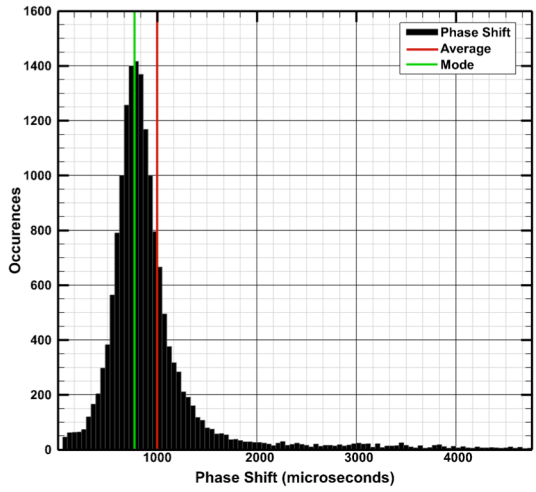


Figure 8: Time for an Unsteady Structure to Traverse from Transducer 1 to Transducer 2, Histogram

The fractional speed at which structures are rotating in the rim seal cavity is calculated using Equation (1). The structures are found to be rotating at 77.5% of the rotor speed. This is close to the value of 80% reported by Jakoby et al. [2]. It is slower than the rotational speeds recorded by Julien et al. [3] and 87% by Wang et al. [4]. The speed at which the structures rotate is dependent on the geometry of the rim seal cavity and is always recorded as a significant fraction of the rotor speed, but never faster than the rotor rotational speed.

The number of structures within the rim seal cavity is calculated using Equation (2). The number of structures found in the rim seal cavity is calculated to 14.89, which is rounded up to 15. The number of structures is exceedingly dependent on the geometry of the rim seal cavity. A minimum number of three structures were recorded by Jackoby et al. with a simple axial seal [2], and a larger number of 30 structures were recorded by Julien et al. [3].

COMPUTATIONAL SETUP

In order to computationally simulate the structures found in the rim seal cavity ANSYS CFX (64-bit, version 15) is employed as a transient, unsteady, three dimensional, compressible Reynolds Averaged Navier-Stokes solver. The solver was distributed in parallel mode with as many as 48 license used at a time.

Figure 9 shows geometry representative of the domains from the Meridional view. It is divided into two subdomains, the first being a stationary domain containing the nozzle guide vane, the stator hub, the casing, and the rim seal cavity. The inlet is located one axial vane cord upstream of the leading edge.

The second domain is the rotating domain and it contains the rotor blade, rotor blade casing, and rotor hub. The exit is locat-

ed 1.25 blade axial chords downstream of the trailing edge of the rotor blade.

Stationary surfaces in the figure include the nozzle casing, nozzle hub, stator side of the rim seal cavity, nozzle guide vane surfaces, and rotor casings. The rotating surfaces include the rotor hub, rotor blade surfaces, and rotor side of the rim seal cavity shown in black.

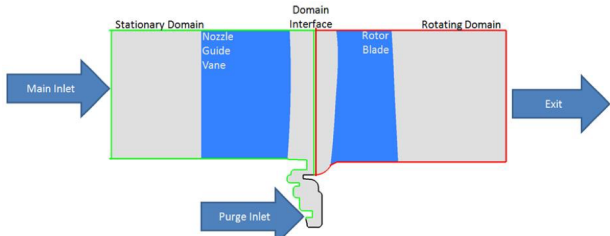


Figure 9: Meridional View of the Computational Domain, Stationary Domain (Green), Rotating Domain (Red)

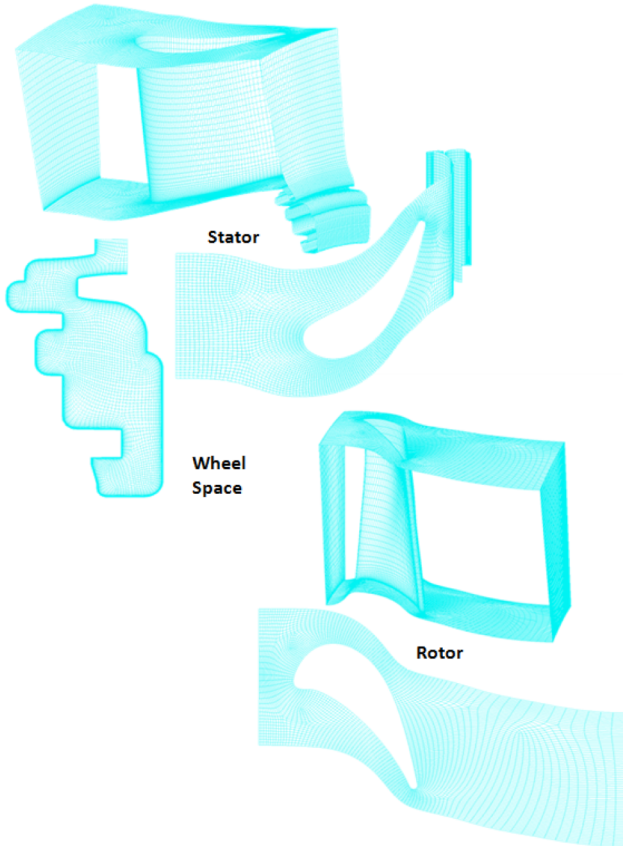


Figure 10: GridPro Generated Structure Grid Surfaces and the Rim Seal Cavity

Grid generation was completed with GridPro. GridPro creates a multi-block, body-fitted, structured, hexahedral grid and uses automated subroutines to improve mesh quality. Figure 10 show the representative geometry of the grid. The stator shown on the top left consists of the vane, hub, casing, inlet outlet, and rim seal cavity. Below and to the right is a detailed view of the

stator hub surface. To the left is an enhanced view of the rim seal cavity. The rotor view consists of the inlet, outlet, hub, casing, and blade surfaces. Below it is a view of the rotor hub surface mesh.

Boundary layers are only placed on the hub surfaces and within the rim seal cavity. Boundary layers are not included on the blade or the casing surfaces as they do not have great effect on the rim seal cavity ingestion and egression. Additionally, no blade tip clearance is used for the rotor.

The size and boundary conditions of the computational domain along with grid independence is recorded in great detail in Averbach [10]. A quick over view of the work will be given here. The resources required to complete a full rotor simulation were not available. There are 29 vanes and 36 blades, a ratio of 0.8056:1. A sector model of 8 vanes and 10 blades is used, a ratio of 0.8:1. The calculated pitch ratio between the sector model and the actual stage is 0.9931.

A domain of sufficient size must be used in order to correctly capture the unsteady structures within the rim seal cavity. From the experimental results, we expect there to be approximately 15 structures. Each structure would be 24° apart from the next structure. The current rim seal cavity simulation contains 99.31° of space and would have the ability to capture 4 of the structures within it.

The unsteady analysis was started by completing a frozen rotor run with stage averaging, which then stepped into the transient simulation. A time step of the required time to move the rotor 1/8th of a blade pitch was chosen, or 1.4481×10^{-4} seconds for the first half of a rotor revolution. Afterward a more fine time step of 1/16th of a blade pitch movement time, or 7.4405×10^{-5} seconds, was used for data gathering. Four blade pitch passages, or 64 time steps are completed with 15 inner loops for each time steps. These four pitch passages are used for the transient results.

COMPUTATIONAL RESULTS

Static pressure in the simulation is monitored at the same radial location as the piezoresistive pressure transducers shown in Figure 1 and Figure 2. Results of the static pressure across the rim seal cavity surface of the first eight vanes are shown in Figure 11.

In Figure 11 a single peak is identified by a green dot. The movement of the rotor is represented by the red line. The variable 't' represents the current time, while 'T' resents the time it takes for the rotor to move one blade pitch. At $t/T=0$ both the green dot and the red line are at the same position. The distance between the green dot and the red line becomes greater as time steps move on. The pressure peak is moving slower than the rotor, as expected. Four pressure peaks are also readily identified in the results. Knowing the numbers of vanes in the domain (8) and the number of vanes in the full stage (29) makes it possible to find the total number of structures in the

simulated stage. The calculation shows that in the simulated stage there are 14.5 unsteady structures.

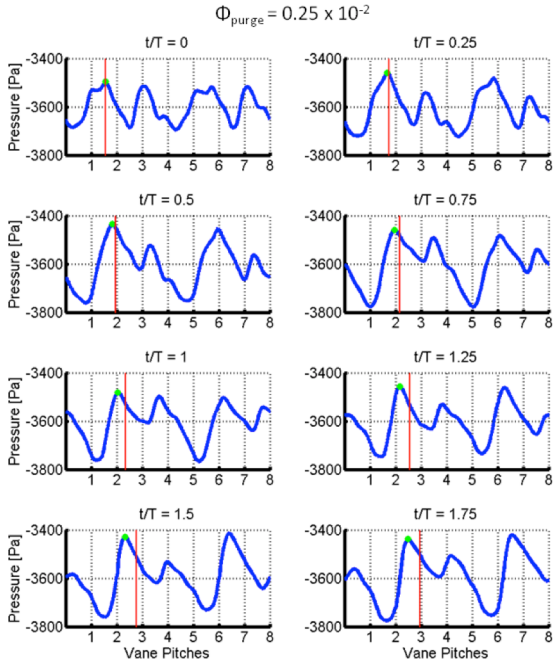


Figure 11: Static Pressure Across the NGV Side Rim Seal Cavity at Varying Time

$$\Omega_{str} = \frac{\theta_{peak,t+1} - \theta_{peak,t}}{\omega_{rotor} \Delta t} \frac{\pi}{180} \quad (4)$$

The speed at which the structures can be calculated using Equation (4). The rotor speed, along with the time step, is set with the initial conditions of the simulation. The four peaks observed in Figure 11 are mapped for the time step and recorded in Figure 12. The figure shows the rotor moving (black dot-dash line) at a constant speed which is greater than the speed of all peaks. The four peaks do not move uniformly and have variance in speed from one step to another. The peaks could be inherently unsteady, or an insufficient number of rotor rotations were used during the simulation before data is collected. The authors opinions are that the structures are, and will continued to be, unsteady during the simulation. The average speed for which the peaks are moving is 81.7% of the rotor speed. This is also the rotational speed at which the unsteady structures are moving.

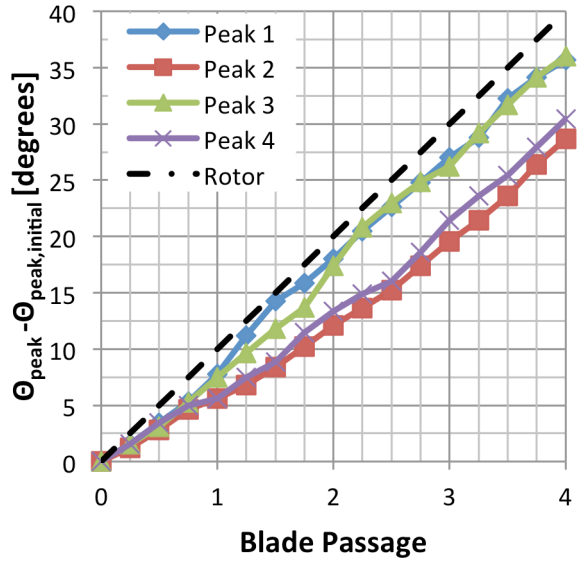


Figure 12: Static Pressure Peak Location

CONCLUSIONS

A test to compare experimental and computational results is proposed. To the author's knowledge, there has been no such experimental analysis using piezoresistive pressure transducers to investigate unsteady cells within the rim seal cavity. A summary of the experimental and computational results can be found in Table 2. The number of cells found experimentally was 15, while the number of cells found in the computation was 14.5. The fractional number of cells is due to the way the rim seal cavity is dependent on the number of vanes used in the simulation (8) and the total number of vanes in the stage (29). There are a prime number of vanes which helps to eliminate vibrations in the system at the cost of increased complexity for the computational analysis. The structures in the rotor are measured experimentally to be moving at 77.5% rotor speed, while the structures in the computational study are found to be moving at 81.7% rotor speed. Results are found to be within good agreement.

Table 2: Results of Experimental and Computational Analysis of Unsteady Cells within the Rim Seal Cavity

	Experimental	CFD
Number of Cells	15	14.5
Cell Speed/Rotor Speed	77.5%	81.7%

The computational results would benefit from a full rotor simulation with an increased number of revolutions during the transient phase. The larger domain would allow more structures to develop. The increased number of revolutions would allow the structures to develop more and settle. The experimental results would benefit from increased scrutiny into the measured data sets. The averaged results compare favorably to the URANS

code. However, URANS by definition will average, the structures maybe inherently unsteady and could not ever settle down to a steady state solution. A more in depth look into the results from the piezoresistive transducers may reveal that the structures with are changing in size, shape, and periodicity even after steady state operation of the turbine has been reached.

ACKNOWLEDGMENTS

The Turbomachinery Aero-Heat Transfer Laboratory at The Pennsylvania State University would like to thank Ozhan Turgut for his guidance in meshing and CFD operation, Harry Houtz and Nick Doroschenko for their expertise in all things probe and mechanical, and our sponsors NASA National Research Announcement and Pratt and Whitney Aircraft Engines.

References

- [1] C. Cao, J. W. Chew, P. R. Millington and S. I. Hogg, "Interaction of Rim Seal and Annulus Flows in an Axial Flow Turbine," in *Proceedings of the ASME Turbo Expo 2003*, Atlanta, 2003.
- [2] R. Jakoby, T. Zierer, K. Lindblad, J. Larsson, L. deVito, D. E. Bohn, J. Funcke and A. Decker, "Numerical Simulation of the Unsteady Flow Field in an Axial Gas Turbine Rim Seal Configuration," in *IGTI2004-53829*, Vienna, 2004.
- [3] S. Julien, J. Lefrancois, G. Dumas, G. Boutet-Blais, S. Lapointe, J.-F. Caron and R. Marini, "Simulations of Flow Ingestion and Related Structures in a Turbine Disk Cavity," in *IGTI2010*, Glasgow, 2010.
- [4] C.-Z. Wang, B. V. Johnson, S. P. Mathiyalagan, J. A. Glahn and D. F. Cloud, "Rim Seal Ingestion in a Turbine Stage from 360-Degree Time-Dependant Numerical Simulations," in *IGTI2012-6*, Copenhagen, 2012.
- [5] A. V. Mirzamoghadam, S. Kanjiyani, A. Riahi, R. Vishnumolakala and L. Gundeti, "Unsteady 360 CFD Validation of a Turbine Stage Mainstream/Disc Cavity Interaction," in *IGTI2014-25466*, Dusseldorf, 2014.
- [6] P. Palaflox, Z. Ding, J. Bailey, T. Vanduser, K. Kirtley, K. Moore and R. Chupp, "A New 1.5-Stage Turbine Wheelspace Hot GAs Ingestion Righ (HGIR) - Part I: Experimental Test Vehicle, Measurement Capability and Baseline Results," in *IGTI2013-96020*, San Antonio, 2013.
- [7] A. M. Basol, A. Raheem, M. Huber and R. S. Abhari, "Full-Annular Numerical Investigation of the Rim Seal Cavity Flows Using GPU's," *IGTI2014-26755*, Dusseldorf, 2014.
- [8] C. McClean, C. Camci and B. Glezer, "Mainstream Aerodynamic Effects Due to Wheelspace Coolant Injection in a High-Pressure Turbine Stage: Part I-Aerodynamic Measurements in the Stationary Frame," *Transaction of the ASME, Journal of Turbomachinery*, vol. 123, no. 4, pp. 687-696, 2001.
- [9] C. McClean, C. Camci and B. Glezer, "Mainstream Aerodynamic Effects due to Wheel Space Coolant Injection in a High Pressure Turbine Stage, Part-II Rotational Frame Measurements," *Transactions of the ASME, Journal of Turbomachinery*, vol. 123, no. 4, pp. 697-703, 2001.
- [10] M. Averbach, Simulation and Experimental Validation of the Wheel Space of the Axial Flow Turbine Research Facility Under Low Purge Flow Conditions, University Park: The Pennsylvania State University The Graduate School, 2014.
- [11] P. Palaflox, Z. Ding, K. Moore, R. Chupp and K. Kirtley, "A New 1.5-Stage Turbine Wheelspace Hot Gas Ingestion Rig (HGIR) - Part II: CFD Modeling and Validation," in *IGTI2013-96021*, San Antonio, 2013.